ACS APPLIED MATERIALS & INTERFACES

Research Article

www.acsami.org

Effect of Substrates on the Photoelectrochemical Reduction of Water over Cathodically Electrodeposited p-Type Cu_2O Thin Films

Sanjib Shyamal,[†] Paramita Hajra,[†] Harahari Mandal,[†] Jitendra Kumar Singh,[‡] Ashis Kumar Satpati,[§] Surojit Pande,[∥] and Chinmoy Bhattacharya*[,†]

[†]Department of Chemistry, Indian Institute of Engineering Science & Technology (IIEST), Shibpur, Howrah 711 103, West Bengal, India

[‡]Corrosion & Surface Engineering CSIR, National Metallurgical Laboratory, Jamshedpur 831007, India

[§]Analytical Chemistry Division, Bhabha Atomic Research Centre, Trombay, Mumbai 400085, India

[∥]Birla Institute of Technology & Science (BITS), Pilani 333031, Rajasthan, India

Supporting Information

ABSTRACT: In this study, we demonstrate development of p-Cu_2O thin films through cathodic electrodeposition technique at constant current of 0.1 mA/cm^2 on Cu, Al, and indium tin oxide (ITO) substrates from basic $CuSO_4$ solution containing Triton X-100 as the surfactant at 30−35 °C. The optical and morphological characterizations of the semiconductors have been carried out using UV−vis spectroscopy, X-ray diffraction (XRD), scanning electron microscopy (SEM), and Raman spectroscopy. The band gap energy of ∼2.1 eV is recorded, whereas SEM reveals that the surface morphology is covered with Cu_2O semiconductors. XRD analyses confirm that with change in substrate, the size of Cu_2O "cubic" crystallites decreases from ITO to Al to Cu substrates. Photoelectrochemical characterizations under dark and illuminated conditions have been carried out through linear sweep voltammetry, chronoamperometry and electrochemical impedance spectroscopic analysis. The photoelectrochemical reduction of water ($H_2O \rightarrow H_2$) in pH 4.9 aqueous solutions over the different substrates vary in the order of Cu > Al > ITO. The highest current of 4.6 mA/cm^2 has been recorded over the Cu substrate even at a low illumination of 35 mW/cm^2, which is significantly higher than the values (2.4 mA/cm^2 on Au coated FTO or 4.07 mA/cm^2 on Cu foil substrate at an illumination of 100 mW/cm^2) reported in literature.

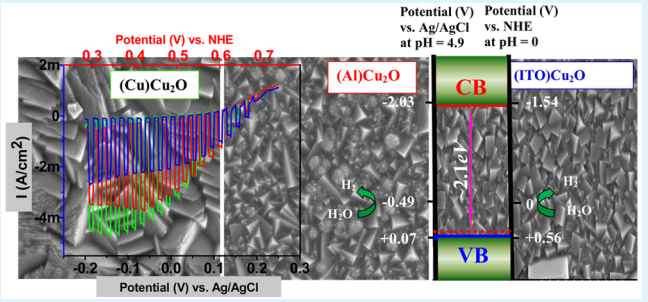

KEYWORDS: *semiconductor photoelectrochemistry, cathodic electrodeposition, electrochemical impedance spectroscopy, action spectra, ohmic conductivity, photoelectrochemical reduction of water*

1. INTRODUCTION

The present paper reports the synthesis of an efficient p-type photocatalyst that may sufficiently use solar energy to drive the $H_2O \rightarrow H_2$ reaction. Cuprous oxide (Cu_2O) thin films were grown on different substrates as Cu foil, Al foil, and indium tin oxide (ITO) coated glass, through galvanostatic electrodeposition technique at various temperatures from a basic $CuSO_4$ solution. Cu_2O is one of the promising metal oxides for applications in solar-energy conversion, electrode materials, sensor and catalysis. The material generally shows p-type semiconductivity[1−3] due to the presence of copper (cation) vacancies within the metal oxide crystal.[4] It has also many important characteristics, such as low production cost and low toxicity.[5]

The possibility of producing hydrogen using UV light was first demonstrated by Fujishima and Honda in 1972 using titanium dioxide as the semiconductor material.[6] Hydrogen evolution[7,8] from renewable sources such as sunlight and water will be quite important when fossil fuel supplies become depleted or when the environmental consequences of burning fossil fuels are no longer acceptable. In this context, p-type Cu_2O is considered to be a potential material that produces hydrogen through splitting of water by using sunlight, because of the favorable band energy positions, with a predicted flat band potential ∼0.2 V positive to the hydrogen evolution reaction.

The galvanostatic deposition of p-type Cu_2O thin film over the conducting glass substrate from a basic $CuSO_4$ solution has been demonstrated earlier.[9,10] In the present study, we have employed the cathodic electrodeposition technique in the presence of surfactant to develop the Cu_2O thin film on different conducting materials and investigate the effect of change in substrates, from ITO glass to Cu or Al foil as

Received: May 13, 2015
Accepted: August 5, 2015
Published: August 5, 2015

DOI: 10.1021/acsami.5b04116
ACS Appl. Mater. Interfaces 2015, 7, 18344−18352

composite (Cu)Cu_2O, (Al)Cu_2O, and (ITO)Cu_2O photocatalysts, on the photocatalytic activities.

In comparison with other techniques, electrodeposition has been preferred in the present studies because this technique provide numerous advantages, including (1) it involves relatively simple and inexpensive equipment; (2) deposition is achieved within a very short period of time; (3) films may be fabricated on large and irregular surfaces; (4) thin layer grown by this technique is uniform and homogeneous; (5) nanocrystalline deposits may be easily obtained; (6) the deposition occurs closer to equilibrium than in many high-temperature methods, and interelement diffusion is not a problem; and (7) the toxic gaseous precursors do not have to be used unlike in chemical gas phase methods. More importantly, the easily synthesized compound semiconductor thin films which can be used directly as photoelectrode in the PEC solar cells. As a result, the synthesized Cu_2O thin films exhibit superior performance for solar driven water reduction process when compared with the earlier reported work, and are presented in Table S1, (Supporting Information). To our knowledge, this is one of the best reports of utilizing PEC water reduction ($H_2O \rightarrow H_2$) on as-prepared Cu_2O thin film under minimum illumination of UV−vis. light.

Because the metallic Cu itself plays an irreplaceable role in modern electronic circuits due to its excellent electrical conductivity, the heterojunction of (Cu)Cu_2O can enhance the photocatalytic property of Cu_2O-based semiconductors. It has been reported that the existence of the metallic substrate (e.g., Cu) may promptly transfer photogenerated charge carriers, avoiding the recombination of electron−hole pairs in the semiconductor matrix.[11] Therefore, the Cu_2O film deposited onto low cost substrates as Cu and a similar surface, Al foil, may act as the potential candidate for direct water splitting for H_2 production as well as in the photodecomposition of organic pollutants. PEC performances regarding $H_2O \rightarrow H_2$ reaction by the Cu_2O electrodes on different substrates were evaluated through linear sweep voltammetry (LSV), chronoamperometry, photocurrent action spectra, and calculation of the incident photon to current conversion efficiency (IPCE) and absorbed photon to current conversion efficiency (APCE) measurements. UV−visible absorption, electrochemical impedance spectra (EIS), Raman spectroscopy, X-ray diffraction (XRD), and scanning electron microscopy (SEM) were employed for physical and surface characterization of the various Cu_2O thin films to explain the role of the substrates on the PEC performance of the materials.

2. EXPERIMENTAL SECTION

2.1. Materials. All the chemicals (AR grade), namely, copper sulfate, dipotassium hydrogen phosphate, potassium hydroxide, sodium sulfate, sodium acetate, acetic acid and lactic acid, were purchased commercially (Emerck) and were used in the as-received condition. The metal precursor solutions were prepared in Milli-Q grade water. ITO coated glass (~15 Ω/sq cm, Xin Yan Technologies, Hong Kong), Cu foil (purity >99.9%) and Al foil (purity >99.9%) were used as substrates to prepare thin films after suitable cleaning procedures.[12]

2.2. Preparation of Deposition Bath. The deposition bath was prepared with 0.2 M copper sulfate and 3 M lactic acid solution in water in the presence of 0.5 M dipotassium hydrogen phosphate buffer and 1% Triton X-100 (TX-100). The pH of the solution was maintained at 12−13 with dropwise addition of 2 M KOH solution. The basic pH value was used to ensure that the deposited Cu_2O was of p-type in nature, whereas it was observed that Cu_2O deposited in acidic pH value exhibited n-type behavior.[13]

2.3. Cu_2O Electrodeposition. The Cu_2O thin films were electrodeposited from a basic solution of lactate stabilized copper sulfate on different substrates using a source-meter (Metravi, India). In the two electrode configuration cell, a large area Pt foil was used as the anode compartment, whereas the ITO coated glass/Cu/Al foil substrate was used as the cathode compartment. The temperature of the deposition bath varied from 10 to 70 °C using thermostat. The optimized growth of the Cu_2O thin film was maintained at a temperature of 30−35 °C for 210 min of deposition at constant applied current of −0.1 mA/cm^2.

2.4. Physicochemical Characterization. Absorption spectra of the thin film semiconductors were carried out using a V-630 UV−vis spectrophotometer (Jasco, Japan) and from the absorption edge, band gap energy was calculated. It is to be noted that absorbance of the Cu_2O films developed over metallic Cu and Al substrates could not be measured separately and are considered to be similar to that over the ITO coated glass substrate, as all the films appeared to be of similar nature. The crystalline behavior of the Cu_2O semiconductor was identified through the powder X-ray diffraction (XRD) measurement using a Bruker AXS D8 Discover Diffractometer (Bruker AXS, Karlsruhe, Germany), operated with a Cu Kα source (λ = 1.54 Å), and the data were recorded with a scan rate of 2° min^{-1} within the 2θ range of 20−80°. Raman spectroscopy was performed by using Almega dispersive micro Raman spectroscope (Thermo Electron Corp. Ltd., Waltham, MA) by exciting the beam of Nd YAG laser (λ = 532 nm) on the samples. The power of the laser was kept low to avoid the transformation of phases because of local heating effect. The locations of the samples were focused through an Olympus microscope at the magnification of 50×. The motorized sample holder platform with Jokey to have fine focusing and mapping at a suitable desired portion of the samples. The grating was 672 lines mm^{-1}, 25 μm pinhole. Prior to analysis of the samples, the instrument was calibrated by using pure Silicon at the peak of 520 cm^{-1}. The surface morphology of the Cu_2O thin film on various substrates was observed through scanning electron microscopy (SEM) using JEOL S4800 FESEM.

2.5. Capacitance Measurements (Mott−Schottky Analysis). Capacitance measurements were carried out using Autolab-302, PG-Stat, FRA-II (Metrohm, The Netherlands) in a borosilicate glass cell with three-electrode configuration containing a Pt rod counter and a standard Ag/AgCl as the reference electrode. In the present report, the working potential vs Ag/AgCl was converted to NHE using Nernst's equation. The Cu_2O thin film exposed through an O-ring, of surface area 0.27 cm^2, was used as the working electrode. An acetate buffer (pH 4.9) with 0.1 M Na_2SO_4 was used as working solution to study the behavior of the semiconductor-electrolyte interface. Measurements were done within the potential range of 0.38−0.58 V vs NHE using ac RMS amplitude of 10 mV with four different frequencies of 200, 500, 1000, and 10000 Hz. Effect of film thickness on the Mott−Schottky analysis was verified by carrying out the experiment using Cu_2O film deposited on Cu substrate with different time interval (60, 120, 180, and 210 min of deposition).

2.6. Photoelectrochemical Measurements. The photoelectrochemical water reduction reaction ($H_2O \rightarrow H_2$) over the prepared semiconductor thin film working electrode surface was carried out in the similar electrochemical cell, as stated above using the CHI-650 potentiostat (CH Instruments, Austin, TX). Linear sweep voltammetry was done within the potential range of 0.73−0.28 V vs NHE with a scan rate of 10 mV/s. The above potential ranges have been selected for PEC measurement in order to avoid the degradation of the Cu_2O semiconductor film, as reported earlier.[14,15] The photoresponse was measured under periodic chopped irradiation from Xe-arc lamp (35W, Hamaan, India) as a white-light source with an incident beam intensity of 35 mW/cm^2. The PEC measurements of these electrodes were carried out with a 0.27 cm^2 geometric area exposure (using O-ring of the same inner area) to the electrolyte solution under light irradiation. A 420 nm cutoff filter (Oriel, Irvine, CA) was used for visible irradiation. The electrolyte was 0.1 M Na_2SO_4 solution in 0.2 M

DOI: 10.1021/acsami.5b04116
ACS Appl. Mater. Interfaces 2015, 7, 18344−18352

sodium acetate buffer (pH 4.9). In all photoelectrochemical experiments, the working electrode was illuminated through the electrolyte/electrode interface. Effect of film thickness on the photoelectrochemical reduction of water was verified by carrying out the experiment using Cu_2O film deposited with different time interval, as stated earlier, on Cu substrate.

Stability of the semiconductors undergoing photoelectrochemical H_2 evolution reaction in the same solution, as stated above, was determined through chronoamperometry at a fixed potential of 0.33 V vs NHE, using the similar cell configuration under constant illumination of 35 mW/cm^2. The results were subsequently verified through calculation of percent of decrease in photocurrent in repeated LSV scan under illumination using the same photoelectrode. PEC action spectrum was determined through chronoamperometry under periodic illumination using a monochromator (Oriel, Irvine, CA). Incident photon or absorbed photon to current conversion efficiencies (IPCE or APCE) were calculated from the optical power of the monochromatic incident beam and absorbance of the semiconductor, respectively.

Photoelectrochemical reduction of the "sacrificial reagent" namely, methyl viologen ($MVCl_2$) was carried out to identify the photoreduction products as well as stability of the Cu_2O thin film undergoing photoelectrochemical processes. Solution containing 0.01 M of the MV^{2+} in 0.1 M Na_2SO_4 (pH 7 phosphate buffer solution) as supporting electrolyte was used in the three electrode cell with the Cu_2O thin film acts as the photocathode. A constant potential of −0.06 V vs NHE was applied under dark followed by illuminated condition, and the gradual color change of the surface was recorded.

2.7. Electrochemical Impedance Measurements (Nyquist Analysis). The electrochemical impedance measurements were carried out under dark, visible and UV−visible illumination with the help of same AUTOLAB with an applied potential of 0.33 V vs NHE reference electrode within the frequency range of 100 kHz to 20 mHz using ac RMS amplitude of 10 mV using the same electrolytic solution.

3. RESULTS AND DISCUSSION

To improve the photocatalytic activity of p-type Cu_2O semiconductors, different substrates were used. The applications of different substrates on which thin films were developed have an influence on its overall photocatalytic behavior in different ways. Among these, the important factors are believed to be (1) modification of the surface morphology of the semiconductor (SC), (2) variation in ohmic contact with the substrate to the SC, (3) change in carrier concentration, and (4) change in carrier mobility. Variation of potential with time during the electrodeposition process has been presented in Figure S1 (Supporting Information). From the figure, it is evident that the deposition process became stable at a faster rate (within 400−500 s of deposition) over Cu foil followed by the ITO coated glass substrate (2400−2500 s). For Cu_2O deposition over the Al surface the galvanic effect between Al^0 and Cu^+ (generated through cathodic reduction of $Cu^{2+} \rightarrow Cu^+$) leads to the formation of Cu_2O semiconductor as well as elemental Cu over the electrode surface. It has been observed that during the deposition of Cu_2O over Al surface, after an initial period of ∼3000 s the concentration of the Cu^{2+} ions near the electrode surface drop down significantly because of the consecutive reactions of $Cu^{2+} \rightarrow Cu^+$ and $Cu^+ \rightarrow Cu^0$, leading to the sharp fluctuation in the electrode potential. These processes continue until next 3000−3500 s after that the process becomes stabilized.

3.1. Physicochemical Characterization. The nature of the deposited materials has been revealed through scanning electron microscopic analysis. Figure 1 shows SEM images for the Cu_2O materials when grown on metallic Cu, Al, and ITO-coated glass substrates. The presence of "cubic" shaped

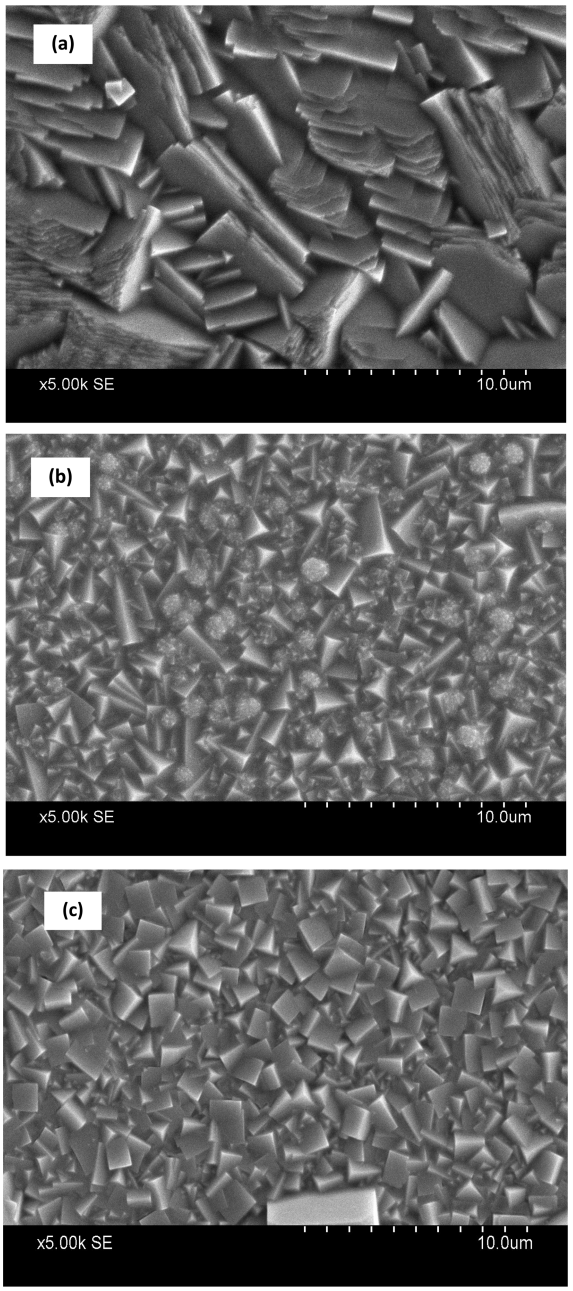

Figure 1. SEM images of Cu_2O thin film (deposition condition: applied current density, −0.1 mA/cm^2; bath temperature, 30 °C; in pH 12 buffer solution) on different substrates: (a) Cu foil, (b) Al foil, and (c) ITO-coated glass.

materials has been confirmed over all of the substrates. From Figure 1a, it is evident that compact forms of well-defined cubes are covered over the Cu surface compared with other two substrates. Presence of smaller "seeds" almost throughout the surface of the materials grown over ITO-coated glass indicates unfavorable support of the substrate for electrodeposition, which affect their overall photoelectrochemical performance. The difference in surface morphology with the change in substrate may be explained by the facts that metallic Cu with highest electrical conductivity (better ohmic contact) favors growth of electrodeposited Cu_2O onto its surface and that the surface morphology is found to be covered with well grown particles. Conductivity of Al is somehow lower than that of Cu, which also favors the growth to some extent, and thus, a

DOI: 10.1021/acsami.5b04116
ACS Appl. Mater. Interfaces 2015, 7, 18344−18352

significant number of "peaks" of Cu_2O cubes is clearly visible over the surface. The lower conductivity of the ITO glass limits the growth of electrodeposited Cu_2O semiconductors showing relatively fewer cubes over the surface.

Crystalline properties of the as deposited Cu_2O on different substrates (Cu, Al and ITO coated glass) were investigated through X-ray diffraction (XRD) analysis. Figure 2a represents

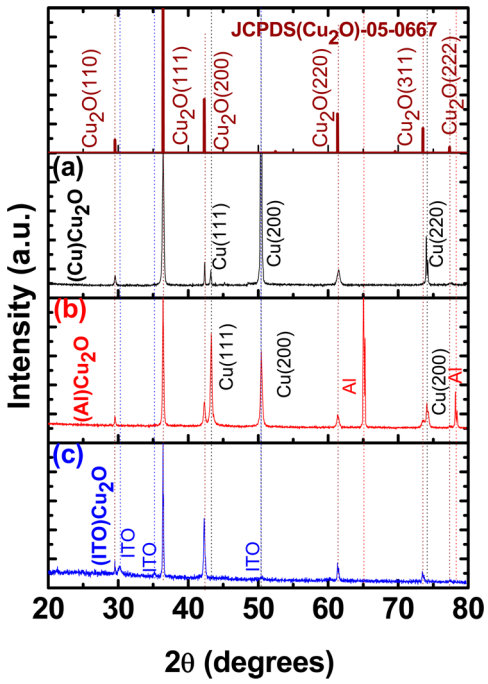

Figure 2. X-ray diffraction pattern of Cu_2O thin film on (a) Cu foil, (b) Al foil, and (c) ITO-coated glass substrate.

the XRD pattern of the $(Cu)Cu_2O$ film, that indicates along with three peaks (at 2θ = 42, 51, and 75°) for elemental Cu coming from the Cu substrate (Supporting Information Figure S2), all others are attributed to the cubic Cu_2O (Standard JCPDS file no. 05-0667) with a strong (111) orientation, without traces of CuO or $Cu(OH)_2$ being identified. In the XRD pattern of $(Al)Cu_2O$ film, as presented in Figure 2b, more numbers of peaks, compared with other substrates, are observed. These peaks are attributed to the elemental Al, arising from the Al substrate (Supporting Information, Figure S2), along with "regular" peaks attributed to deposited Cu_2O semiconductor and three more peaks generated from Cu^0. Presence of elemental Cu in the $(Al)Cu_2O$ semiconductor are attributed to the fact that Cu^+ as generated through the primary electrolytic reduction of Cu^{2+} may undergo secondary galvanic reduction reaction within the deposition bath between metallic Al substrate and Cu^+ ($Al \rightarrow Al^{3+} + 3e^-$ and $Cu^+ + e^- \rightarrow Cu^0$) and is not possible for the ITO coated glass substrate. Figure 2c represents the XRD plot of the thin film semiconductor on conducting glass substrate showing similar patterns of Cu_2O with the strongest (111) orientation along with three peaks arising from ITO substrate and has been presented in Figure S2, Supporting Information.

The relative trend in crystallinity of Cu_2O in three different substrates reveals that the individual peak positions and their relative intensities are in good agreement with that of the cubic forms with strong (111) orientation. The only change of XRD patterns of Cu_2O with change the substrate is that the ratio of peak intensity between two peaks (111) and (200) has changed from 4.08 for Cu substrate to 3.51 for Al and 3.12 for ITO substrates. The sizes of the Cu_2O crystallites (D in Å) were calculated using the Scherrer equation[16] for three substrates and are found in the order of 31 nm for $(Cu)Cu_2O$, 36 nm for $(Al)Cu_2O$, and 45 nm for $(ITO)Cu_2O$.

$$D = (0.9\lambda)/\beta\cos\theta \quad (1)$$

where λ is the X-ray wavelength(1.541 Å), β is fwhm (full width at half maxima, in degrees), θ is the diffraction angle (in degrees). The trend in crystallite size of Cu_2O over different substrates may be ascribed to higher ohmic conductivity of the Cu foil than that for Al foil or ITO coated glass substrates.

The influence of substrates on the structural formation of Cu_2O thin films were further studied through Raman Scattering analysis. Figure 3 shows the Raman dispersion spectra of the

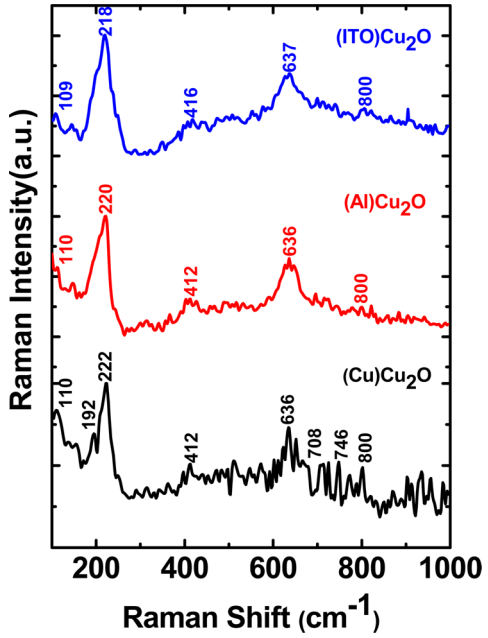

Figure 3. Raman scattering of Cu_2O thin film on different substrates.

semiconductor thin films on different substrates indicating the characteristic phonon frequencies of crystalline Cu_2O. The most intense peak originated at 218 cm^{-1} for the sample deposited on ITO coated glass substrate and is attributed to the second-order Raman-allowed mode ($2\ \Gamma_{12}^-$) of Cu_2O. However, the same peak shifted to 220 and 222 cm^{-1} for the Al and Cu substrate, respectively. The sharply defined mode of the strongest peaks demonstrated the high structural quality of the synthesized samples. The peak at 109 ± 1 cm^{-1} is assigned to the inactive Raman mode.[17] The weak peak at 416 cm^{-1} is assigned to four phonon mode ($3\ \Gamma_{12}^- + \Gamma_{25}^-$),[18]; however, this peak shifted to 412 cm^{-1} for Cu and Al substrates. A moderate peak at 636 cm^{-1} is marked to the red-allowed mode.[19] The characteristic peaks of CuO under the same experimental conditions at 298, 330, and 602 cm^{-1} could not be detected and therefore suggests that the Cu_2O film is free of this contaminant, as was confirmed in XRD analysis.

UV−visible measurements were carried out using as-prepared thin films to calculate the band gap energies. Figure 4 shows the UV−visible absorption spectra of Cu_2O thin films deposited on ITO glass substrate with an applied cathodic

DOI: 10.1021/acsami.5b04116
ACS Appl. Mater. Interfaces 2015, 7, 18344−18352

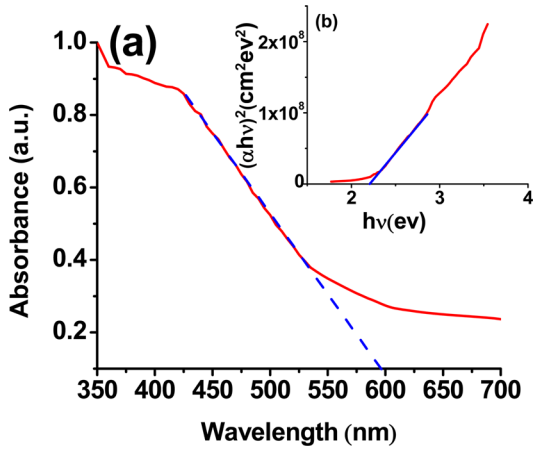

Figure 4. (a) UV − visible absorption spectra of electrodeposited Cu_2O thin film on ITO-coated glass substrate and (b) Tauc plot of the same film.

current density of 0.1 mA/cm^2 at a constant temperature of 30 °C and pH 12 conditions. From the spectra, a sharp absorption band is observed for the films indicating the onset of the absorption edge near to 600 nm corresponding to the band gap energy of ∼2.1 eV of the as deposited Cu_2O semiconductor and is in good agreement with that reported in the literature.[20]

3.2. Capacitance Measurements. To determine the nature of the semiconductors, flat band potential, and carrier concentrations, we subjected the Cu_2O thin films on different substrates to electrochemical impedance spectroscopic analysis through Mott−Schottky plot and are represented in Figure 5.

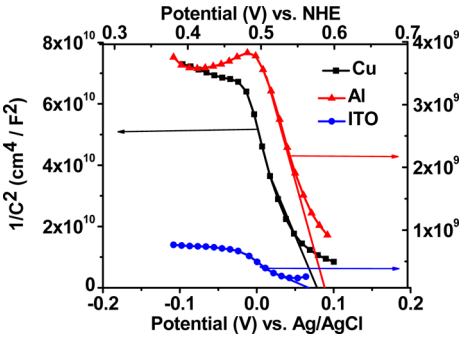

Figure 5. Mott−Schottky plots of Cu_2O film on different substrates in the presence of 0.1 M Na_2SO_4−acetate buffer solution (pH 4.9) using an ac frequency of 1000 Hz.

Experiments were carried out in 0.1 M Na_2SO_4 acetate buffer solution at different frequencies (200, 500, 1000, and 10000 Hz) within the potential region of 0.38−0.58 V vs NHE reference electrode. Variation of capacitance (C) with applied potential may be represented by the Mott−Schottky equation,[21] eq 2

$$1/C_{sc}^2 = (2/e\varepsilon\varepsilon_0 N_A)(E - E_{fb} - kT/e) \quad (2)$$

where C_{sc} is the space-charge capacitance (in F/cm^2), e is the electronic charge (C); ε is the dielectric constant of the semiconductors;[22] ε_0 is the permittivity of free space; N_A is the carrier density in cm^{-3}; E is the applied potential (V); E_{fb} is the flat band potential (V); k is the Boltzmann constant; and T is the temperature (K). The negative slope of the plot confirms the p-type behavior of the Cu_2O semiconductor, and the acceptor density was calculated and found to be of the order of 3.26×10^{20} cm^{-3} for ITO substrate, 9.33×10^{19} cm^{-3} for Al substrate and 4.24×10^{18} cm^{-3} for Cu substrate. The flat band potential of the semiconductor on different substrates at a fixed frequency (1000 Hz), as calculated from the intercept on the potential axis of the Mott−Schottky plot, was found to be ∼0.55 ± 0.01 V vs NHE reference electrode that indicates the flat band potential remains almost invariant with change in the substrates. For the same substrate, the flat-band potential is found to be of frequency independent character and is shown in Figure S3 (Supporting Information).

Measurements of band gap energy led to the calculation of the energy band diagram of p-type Cu_2O in pH 4.9 solution and are presented in Figure 6. Position of the conduction band

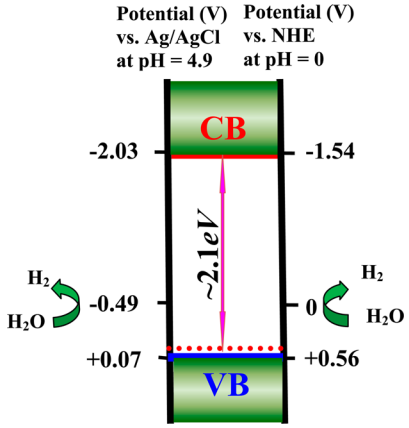

Figure 6. Band diagram of the p-Cu_2O semiconductor-electrolyte interface.

(CB) at −1.54 V vs normal hydrogen electrode (NHE) was determined from the flat band potential of the semiconductor and therefore the corresponding valence band (VB) at +0.56 V vs NHE. The redox potential of the photogenerated electrons (−1.54 V vs NHE; ΔG ∼ 149 kJ/mol) is low enough to drive the water reduction reaction ($H_2O \rightarrow H_2$, E° = 0 V vs NHE), and the material exhibits significant photoelectrochemical reduction behavior, as obtained through LSV and IPCE and APCE measurements.

3.3. Photoelectrochemical Measurements. To investigate the effects of the substrates on the semiconductors, we performed photoelectrochemical (PEC) measurements. The PEC behavior of these materials was studied under periodic chopped UV−visible illumination of the incident light for water reduction in the presence of 0.1 M Na_2SO_4 in acetate buffer (pH 4.9). Figure 7 depicts the LSV plots, that is, the variation of photocurrent density of the water reduction reaction over the Cu_2O thin film, deposited from a constant temperature bath of 30 °C, maintained at a pH level of 12 and with an applied current density of −0.1 mA/cm^2, on three different substrates Cu/Al foil and ITO glass.

It has been observed from the LSV plots that the onset potential (V_{on}) varies to some extent with change in the substrates. For instance, the onset potential is +0.63 V for the Cu_2O film on ITO coated glass, whereas for the metal substrates, the V_{on} is shifted to more positive values: + 0.65 V for Cu and +0.69 V (vs NHE) for Al foil. The onset potential can be defined as the potential where the photocurrent starts showing significantly, that is, the photoreduction of $H_2O \rightarrow H_2$ has just started.[23] Higher positive onset potential or more

DOI: 10.1021/acsami.5b04116
ACS Appl. Mater. Interfaces 2015, 7, 18344−18352

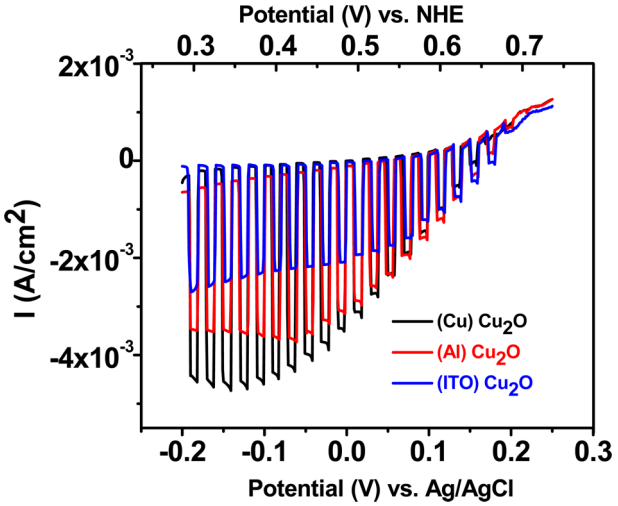

Figure 7. Linear sweep voltammogram (I–V curves) of the p-Cu_2O thin film semiconductor electrode on different substrates in the presence of 0.1 M Na_2SO_4–acetate buffer solution (pH 4.9), under chopped light illumination of 35 mW/cm^2.

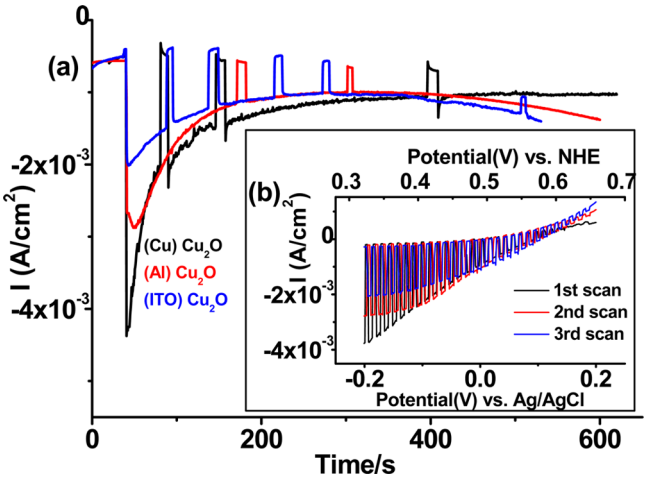

Figure 8. (a) Chronoamperometric plot of the p-Cu_2O thin film semiconductor electrode on different substrates in the presence of 0.1 M Na_2SO_4–acetate buffer solution (pH 4.9) at 0.33 V vs NHE, under continuous illumination of 35 mW/cm^2. (b, inset) Periodic linear sweep voltammogram of the (Cu)Cu_2O thin film semiconductor electrode in the presence of 0.1 M Na_2SO_4–acetate buffer solution (pH 4.9), under chopped light illumination of 35 mW/cm^2.

negative free energy change (ΔG; as $\Delta G = -n$FE and E = V_{oc}), for the reduction reaction indicates the facile charge transfer process over that substrate, that implies the better PEC performance of the material on metallic foils compared with that over the ITO coated glass substrate. The highest photocurrent for the three different samples, as calculated from the LSV plot, was found to be in the order of (Cu)Cu_2O, 4.6 mA/cm^2 > (Al) Cu_2O, 3.7 mA/cm^2 > (ITO)Cu_2O, 2.6 mA/cm^2. When compared with other reported data available in the literature, using electrodeposited Cu_2O, it was observed that the performance of the as prepared semiconductor, measured for photoelectrochemical reduction of water ($H_2O \rightarrow H_2$) current density is the highest, even with a low incident beam intensity of 35 mW/cm^2 only, and the same has been summarized in Table S1 (Supporting Information). Visible responsiveness of the Cu_2O thin film semiconductor toward visible light has been demonstrated through the linear sweep voltammogram. Figure S4 (Supporting Information) represents a typical LSV pattern of the (Cu)Cu_2O thin film undergoing photoelectrochemical reduction of water ($H_2O \rightarrow H_2$) when exposed through the visible and UV–visible light with periodic illumination. Comprehensive visible absorptivity of the material has been confirmed and is in supportive of the band gap energy determination.

Continuous photocurrent was measured for all the materials using the same electrolytic solution when the electrode is held at a constant potential of 0.33 V vs NHE under the steady illumination of 35 mW/cm^2. Figure 8a represents the chronoamperometric plots of the Cu_2O thin film in different substrates showing moderate stability for generation of H_2 from water under illumination. Earlier experiments using Cu_2O semiconductors for photoelectrochemical applications also suggest similar observations on its stability.[24−26] Usability of the semiconductor was tested through periodic voltammetry under chopped illumination (Figure 8b, inset), and it was found with the increase in the number of LSV pattern, the rate of photocurrent decrease is reduced after second successive scans. Scanning electron micrography of the Cu_2O film on Cu substrate after photoelectrochemical studies demonstrates certain modifcations of the surface morphology, as presented in Figure S8 (Supporting Information) and may be considered for the gradual changes in the behavior of the semiconductors film.

Finally, the action spectrum[27−29] for photoelectrochemical reduction of water was recorded through chronoamperometry with change in monochromatic wavelength from 350 to 500 nm, and the corresponding photocurrent at each of the wavelengths was calculated. Incident photon to current conversion efficiency (IPCE) was calculated by measuring the power of the incident light at specified wavelengths. IPCE describes the ratio of "effective photons" that generate electrochemical current across the semiconductor electrolyte interface to "incident photons" of monochromatic light. It is calculated as a function of output photocurrent density (I_{ph}, A/cm^2) and incident light power density (P, W/cm^2) at each wavelength (λ, nm) and is described by eq 3.

$$\text{IPCE}\ (\%) = \frac{I_{ph}}{P_{in}} \times \frac{1240}{\lambda} \times 100 \tag{3}$$

The absorbed photon to current conversion efficiency (APCE) describes the fraction of actual "absorbed photons" by the semiconductor. The relation between IPCE and APCE is shown in eq 4, where A_λ corresponds to the absorbance of the material at any particular wavelength (λ), as measured through UV–visible spectra.

$$\text{APCE}\ (\%) = \left(\frac{\text{IPCE}}{1 - 10^{-A_\lambda}}\right) \times 100 \tag{4}$$

Figure 9 represents the action spectra of Cu_2O thin film on different substrates for water reduction in 0.1 M Na_2SO_4 solution (pH 4.9, acetate buffer solution) when a fixed potential of 0.33 V vs NHE is held under monochromatic illumination. This figure represents the variation of photocurrent with chopped monochromatic light at different wavelengths ranging from 350 to 500 nm, for electrodeposited thin films on different substrates. The corresponding IPCE and APCE, as derived from the respective photocurrent density at each wavelength using eqs 3 and 4, are presented in Figure 10.

DOI: 10.1021/acsami.5b04116
ACS Appl. Mater. Interfaces 2015, 7, 18344−18352

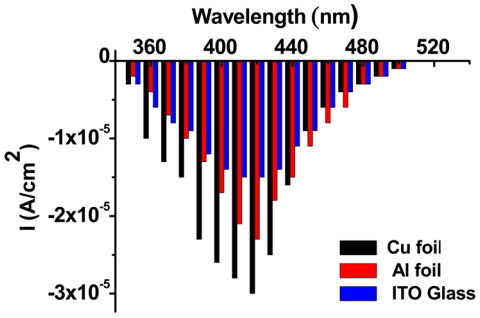

Figure 9. Photocurrent spectrum of p-Cu_2O thin film on different substrates in the presence of 0.1 M Na_2SO_4–acetate buffer solution (pH 4.9) at an applied potential of 0.33 V vs NHE.

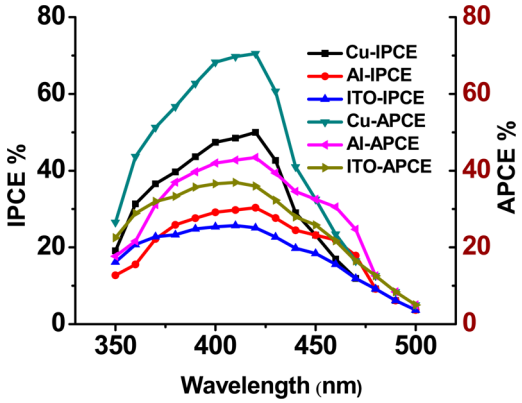

Figure 10. Variation of IPCE and APCE at different wavelengths of the p-Cu_2O thin films on different substrates in the presence of 0.1 M Na_2SO_4 – acetate buffer solution (pH 4.9).

The maximum value of IPCE is 50% and the corresponding APCE value is 70%, was obtained from the Cu_2O film deposited on Cu foil substrate, whereas for Al and ITO glass substrates the highest IPCE values were 30 and 25% and corresponding APCE values were 43 and 37%, respectively. The significant enhancement of photon to current conversion efficiencies for Cu_2O film over the Cu substrate and also to some extent over Al foil demonstrated the superior substrate quality of these metallic elements over conventional ITO coated glass.

Figure S5 (Supporting Information) represents the photograph of the Cu_2O thin film deposited on ITO coated glass substrate immersed in the solution containing MV^{2+} (10 mM) in the presence of 0.1 M Na_2SO_4 (pH 7 phosphate buffer solution) under dark condition when a constant potential of 0.06 V vs NHE was held at the electrode surface. Immediately after the illumination, a deep blue color precipitate was found to develop over the Cu_2O thin film due to the photoreduction of MV^{2+} to methyl viologen cation radical ($MV^{2+}_{colorless} \rightarrow MV^{+\bullet}_{deep\ blue}$) that confirms the photoelectrochemical reduction performance of the as prepared Cu_2O thin film.

3.4. Impedance Measurements. EIS measurements were carried out covering a frequency range of 100 kHz to 20 mHz using an amplitude of 10 mV at a bias potential of 0.33 V vs NHE reference electrode. Figure 11 represents the Nyquist plot for the Cu_2O electrodes prepared on three different substrates under UV–visible illumination. It is known that the high frequency limit of the semicircle in the Nyquist plot is characteristic of the "ohmic" resistance, which, in the present case, is the solution resistance (R_s), whereas the low frequency

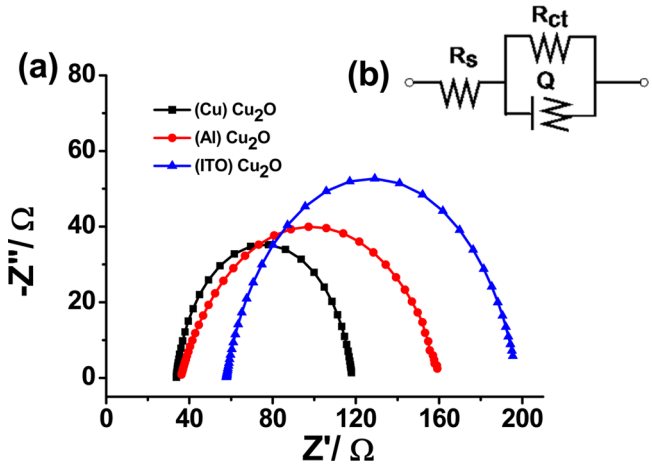

Figure 11. (a) Nyquist plot of the Cu_2O film on different substrates in the presence of 0.1 M Na_2SO_4–acetate buffer solution (pH 4.9) under illumination of 35 mW/cm^2; (b) equivalent circuit model to analyze the Nyquist plot.

limit is the characteristics of the total resistance, that is, the charge transfer resistance (R_{ct}) plus the solution resistance (R_s) and the diameter of the semicircle is equal to the charge transfer resistance (R_{ct}). The variation of the electrochemical impedance parameter has been presented in Table 1. It is

Table 1. Variation of Equivalent Circuit (EC) Parameters of the Cu_2O Thin Film over Different Substrates

sample	R_s (Ω)	R_{ct} (Ω)	Q (CPE) (μF/cm^2)	n
(Cu)Cu_2O	33.4	84.5	482	0.89
(Al)Cu_2O	36.7	125.2	453	0.85
(ITO)Cu_2O	56.8	140.1	300	0.83

evident from the table that the ohmic resistance (R_s) for the different films vary in the order of Cu ≤ Al ≪ ITO. Minimum values of R_s for the films on Cu and Al substrates indicate that the material experiences lower ohmic resistance at the electrode solution interface due to an increase electronic conductivity, better electrical connectivity of Cu_2O semiconductor with metallic Cu and Al substrate as compared with that of ITO coated glass. It is also observed that R_{ct} of Cu_2O thin film varies for different substrates in the order of Cu < Al ≪ ITO under similar experimental conditions, which indicates the facile charge transfer process on metallic Cu substrate and also on Al substrate. However, high R_{ct} on ITO-coated glass indicates less favorable charge transfer process on this electrode because of the slowest mobility of the charge carriers within the bulk of the semiconductor matrix as well as sluggish transfer of charge carriers (in this case, the holes) from the semiconductor to the substrate toward the counter electrode to undergo the counter reaction. It is also evident from the table that the capacitance associated with the constant phase element (CPE) varies in the order of Cu ≥ Al ≫ ITO. Slightly higher capacitive behavior of the semiconductor film on Cu substrate indicates that the semiconductor material is free from any major defects as a whole.

Because the Cu from the substrate may fill up the "defect sites" of the Cu_2O crystallites therefore minimizing acceptor concentration (hole) for a p-type semiconductor and is also evident from the Mott–Schottky analysis of the semiconductor deposited on metallic Cu substrate at different time interval

DOI: 10.1021/acsami.5b04116
ACS Appl. Mater. Interfaces 2015, 7, 18344–18352

(varying film thickness), as presented in Figure S6 (Supporting Information). This also supports the gradual increasing order of photocurrent as obtained from LSV plot of the similar Cu_2O films on Cu substrate, as presented in Figure S7 (Supporting Information). For the Cu_2O deposited on Al, because the substrate facilitates the secondary reduction of Cu^{2+} ($Cu^{2+} \rightarrow Cu^{+} \rightarrow Cu^{0}$) forming elemental Cu in the thin film, that may be incorporated within the defect sites of the Cu_2O lattice thus compensating several holes. The presence of elemental Cu peaks in the XRD pattern of the Cu_2O thin film prepared on Al substrate also supports this observation. Cu_2O thin film prepared on ITO coated substrates are without any chances to reduce the hole concentration by compensating the defect sites, because of unavailability of elemental Cu formation onto the Cu_2O matrix, thereby exhibiting highest "acceptor concentration".

4. CONCLUSION

In this work, we have shown that the cuprous oxide thin films are electrodeposited onto various substrates from an alkaline copper(II) lactate solution at pH 12 with preferred (111) oriented cubic structure. Change in the substrate from ITO-coated glass to metallic Al or Cu foil leads to significant change in the surface morphologies and to a decrease in crystallite size. Among the different substrates, the highest photocurrent of 4.6 mA/cm^2 was observed for Cu substrate, followed by Al and ITO glass substrate under 35 mW/cm^2 illuminations in an aqueous electrolyte (pH 4.9 buffer) for photoelectrochemical reduction of H_2O to H_2. Higher ohmic conductivity of metallic Cu and better substrate properties over the others make it suitable for the development of the efficient photoelectrochemical solar cell. Efficacy of the as-prepared Cu_2O thin film toward conversion of methyl viologen to methyl viologen cation radical ($MV^{2+}_{colorless} \rightarrow MV^{+\bullet}_{deep\ blue}$) confirms the photoelectrochemical reduction performance of the material.

■ ASSOCIATED CONTENT

Supporting Information

The Supporting Information is available free of charge on the ACS Publications website at DOI: 10.1021/acsami.5b04116.

Potential−time variation plot obtained during the galvanostatic deposition process; XRD pattern of the base Cu, Al, and ITO coated glass substrates; Mott−Schottky plot in different frequencies for the (Cu)Cu_2O thin film and LSV pattern for the photoelectrochemical reduction of H_2O under visible and UV−visible illumination using the same electrode, prepared after different deposition times; SEM image of the Cu_2O thin film on Cu foil substrate after photoelectrochemical experimentations; and photoelectrochemical reduction of methyl viologen ($MV^{2+}_{colorless} \rightarrow MV^{+\bullet}_{deep\ blue}$) over the Cu_2O semiconductor electrode and the comparative table, as obtained from literature survey, showing the performance of the Cu_2O thin films in photoelectrochemical reduction of water. (PDF)

■ AUTHOR INFORMATION

Corresponding Author

*E-mail: cbhattacharya.besus@gmail.com.

Notes

The authors declare no competing financial interest.

■ ACKNOWLEDGMENTS

This work was supported by Board of Research in Nuclear Science (BRNS), Department of Atomic Energy, Government of India, sponsored project (ref. No. 2013/37C/61/BRNS/2445, dated 03/12/2013) and the UGC-SAP to the Department of Chemistry, Indian Institute Engineering Science & Technology, Shibpur. We also thank Dr. Malay Kundu of the School of Materials Science & Engineering, IIEST for the SEM characterization.

■ REFERENCES

(1) Toth, R. S.; Kilkson, R.; Trivich, D. Preparation of Large Area Single-Crystal Cuprous Oxide. *J. Appl. Phys.* **1960**, *31*, 1117−1121.

(2) Young, A. P.; Schwartz, C. M. Electrical Conductivity and Thermoelectric Power of Cu_2O. *J. Phys. Chem. Solids* **1969**, *30*, 249−252.

(3) O'Keeffe, M.; Moore, W. J. Electrical Conductivity of Monocrystalline Cuprous Oxide. *J. Chem. Phys.* **1961**, *35*, 1324−1328.

(4) Rakhshani, A. E. Preparation, Characteristics and Photovoltaic Properties of Cuprous Oxide—a review. *Solid-State Electron.* **1986**, *29*, 7−32.

(5) Wei, H. M.; Gong, H. B.; Chen, L.; Zi, M.; Cao, B. Q. Photovoltaic Efficiency Enhancement of Cu_2O Solar Cells Achieved by Controlling Homojunction Orientation and Surface Microstructure. *J. Phys. Chem. C* **2012**, *116*, 10510−10515.

(6) Honda, K.; Fujishima, A. Electrochemical Photolysis of Water at a Semiconductor Electrode. *Nature* **1972**, *238*, 37−38.

(7) Berglund, S. P.; Lee, H. C.; Nunez; Paul, D.; Bard, A. J.; Mullins, C. B. Screening of Transition and Post-Transition Metals to Incorporate into Copper Oxide and Copper Bismuth Oxide for Photoelectrochemical Hydrogen Evolution. *Phys. Chem. Chem. Phys.* **2013**, *15*, 4554−4565.

(8) Yuan, J.; Wen, J.; Gao, Q.; Chen, S.; Li, J.; Li, X.; Fang, Y. Amorphous Co_3O_4 Modified CdS Nanorods with Enhanced Visible-light Photocatalytic H_2-production Activity. *Dalton Trans.* **2015**, *44*, 1680−1689.

(9) Paracchino, A.; Brauer, J.; Moser, J. E.; Thimsen, E.; Graetzel, M. Synthesis and Characterization of High-Photoactivity Electrodeposited Cu_2O Solar Absorber by Photoelectrochemistry and Ultrafast Spectroscopy. *J. Phys. Chem. C* **2012**, *116*, 7341−7350.

(10) Paracchino, A.; Laporte, V.; Sivula, K.; Grätzel, M.; Thimsen, E. Highly Active Oxide Photocathode for Photoelectrochemical Water Reduction. *Nat. Mater.* **2011**, *10*, 456−461.

(11) Zhou, B.; Liu, Z.; Wang, H.; Yang, Y.; Su, W. Experimental Study on Photocatalytic Activity of Cu_2O/Cu Nanocomposites under Visible Light. *Catal. Lett.* **2009**, *132*, 75−80.

(12) Ma, L.; Lin, Y.; Wang, Y.; Li, J.; Wang, E.; Qiu, M.; Yu, Y. Aligned 2-D Nanosheet Cu_2O Film: Oriented Deposition on Cu Foil and Its Photoelectrochemical Property. *J. Phys. Chem. C* **2008**, *112*, 18916−18922.

(13) Wang, L. C.; Tao, M. Fabrication and Characterization of p-n Homojunctions in Cuprous Oxide by Electrochemical Deposition. *Electrochem. Solid-State Lett.* **2007**, *10*, H248−H250.

(14) Wu, L.; Tsui, L.-K.; Swami, N.; Zangari, G. Photoelectrochemical Stability of Electrodeposited Cu_2O Films. *J. Phys. Chem. C* **2010**, *114*, 11551−11556.

(15) de Jongh, P. E.; Vanmaekelergh, D.; Kelly, J. J. Photoelectrochemistry of Electrodeposited Cu_2O. *J. Electrochem. Soc.* **2000**, *147*, 486−489.

(16) Scherrer, P. Bestimmung der Grösse und der inneren Struktur von Kolloidteilchen mittels Röntgenstrahlen. *Nachr. Ges. Wiss. Göttingen* **1918**, *26*, 98−100.

(17) Compaan, A.; Cummins, H. Z. Resonant Quadrupole-Dipole Raman Scattering at the 1S Yellow Exciton in Cu_2O. *Phys. Rev. Lett.* **1973**, *31*, 41−44.

DOI: 10.1021/acsami.5b04116
ACS Appl. Mater. Interfaces 2015, 7, 18344−18352

(18) Yu, P. Y.; Shen, Y. R. Resonance Raman Studies In Cu_2O. I. The Phonon-Assisted D 1*s* Yellow Excitonic Absorption Edge. *Phys. Rev. B* **1975**, *12*, 1377−1380.
(19) Powell, D.; Compaan, A.; Macdonald, J. R.; Forman, R. A. Raman-Scattering Study of Ion-Implantation-Produced Damage in Cu_2O. *Phys. Rev. B* **1975**, *12*, 20−25.
(20) Maijenburg, W. A.; Hattori, A. N.; De Respinis, M.; McShane, C. M.; Choi, K. S.; Dam, B.; Tanaka, H.; ten Elshof, J. E. Ni and p-Cu_2O Nanocubes with a Small Size Distribution by Templated Electrodeposition and Their Characterization by Photocurrent Measurement. *ACS Appl. Mater. Interfaces* **2013**, *5*, 10938−10945.
(21) Bard, A. J.; Faulkner, L. R. *Electrochemical Methods: Fundamentals and Application*, 2nd ed.; John Wiley & Sons: New York, 2001, pp 750−751.
(22) Pei, F.; Wu, S.; Wang, G.; Xu, M.; Wang, S.-Y.; Chen, L.-Y. Electronic and Optical Properties of Noble Metal Oxides M_2O (M = Cu, Ag and Au): First-principles Study. *J. Korean Phys. Soc.* **2009**, *55*, 1243−1249.
(23) Reece, S. Y.; Hamel, J. A.; Sung, K.; Jarvi, T. D.; Esswein, A. J.; Pijpers, J. J. H.; Nocera, D. G. Wireless Solar Water Splitting Using Silicon-Based Semiconductors and Earth-Abundant Catalysts. *Science* **2011**, *334*, 645−648.
(24) Tilley, S. D.; Schreier, M.; Azevedo, J.; Stefi k, M.; Graetzel, M. Ruthenium Oxide Hydrogen Evolution Catalysis on Composite Cuprous Oxide Water-Splitting Photocathodes. *Adv. Funct. Mater.* **2014**, *24*, 303−311.
(25) Zhang, Z.; Wang, P. Highly Stable Copper Oxide Composite as an Effective Photocathode for Water Splitting via a Facile Electrochemical Synthesis Strategy. *J. Mater. Chem.* **2012**, *22*, 2456−2464.
(26) Li, C.; Li, Y.; Delaunay, J.-J. A Novel Method to Synthesize Highly Photoactive Cu_2O Microcrystalline Films for Use in Photoelectrochemical Cells. *ACS Appl. Mater. Interfaces* **2014**, *6*, 480−486.
(27) Bhattacharya, C.; Lee, H. C.; Bard, A. J. Rapid Screening by Scanning Electrochemical Microscopy (SECM) of Dopants for Bi_2WO_6 Improved Photocatalytic Water Oxidation with Zn Doping. *J. Phys. Chem. C* **2013**, *117*, 9633−9640.
(28) Hajra, P.; Shyamal, S.; Mandal, H.; Fageria, P.; Pande, S.; Bhattacharya, C. Photocatalytic Activity of Bi_2O_3 Nanocrystalline Semiconductor Developed Via Chemical-Bath Synthesis. *Electrochim. Acta* **2014**, *123*, 494−500.
(29) Mandal, H.; Shyamal, S.; Hajra, P.; Samanta, B.; Fageria, P.; Pande, S.; Bhattacharya, C. Improved Photoelectrochemical Water Oxidation using Wurtzite ZnO Semiconductors Synthesized through Simple Chemical Bath Reaction. *Electrochim. Acta* **2014**, *141*, 294−301.

NOTE ADDED AFTER ASAP PUBLICATION

This paper was published on the Web on August 13, 2015, with minor text errors. The corrected version was reposted on August 14, 2015.

DOI: 10.1021/acsami.5b04116
ACS Appl. Mater. Interfaces 2015, 7, 18344−18352